9. Scheffold, F., Lenke, R., Tweer, R. & Maret, G. Localization or classical diffusion of light? *Nature* **398,** 206–207 (1999).
10. Weaver, R. L. Anomalous diffusivity and localization of classical waves in disordered media: The effect of dissipation. *Phys. Rev. B* **47,** 1077–1080 (1993).
11. Yosefin, M. Localization in absorbing media. *Europhys. Lett.* **25,** 675–680 (1994).
12. Abrahams, E., Anderson P. W., Licciardello, D. C. & Ramakrishnan, T. V. Scaling theory of localization: absence of quantum diffusion in two dimensions. *Phys. Rev. Lett.* **42,** 673–676 (1979).
13. Landauer, R. Electrical resistance of disordered one-dimensional lattices. *Philos. Mag.* **21,** 863–867 (1970).
14. van Rossum, M. C. W. & Nieuwenhuizen, Th. M. Multiple scattering of classical waves: microscopy, mesoscopy, and diffusion. *Rev. Mod. Phys.* **71,** 313–372 (1999).
15. Kogan, E. & Kaveh, M. Random-matrix-theory approach to the intensity distributions of waves propagating in a random medium. *Phys. Rev. B* **52,** R3813–R3815 (1995).
16. van Langen, S. A., Brouwer, P. W. & Beenakker, C. W. J. Nonperturbative calculation of the probability distribution of plane-wave transmission through a disordered waveguide. *Phys. Rev. E* **53,** R1344–R1347 (1996).
17. Thouless, D. J. Maximum metallic resistance in thin wires. *Phys. Rev. Lett.* **39,** 1167–1169 (1977).
18. Shapiro, B. Scaling properties of probability distributions in disordered systems. *Philos. Mag. B* **56,** 1031–1044 (1989).
19. Stoytchev, M. & Genack, A. Z. Measurement of the probability distribution of total transmission in random waveguides. *Phys. Rev. Lett.* **79,** 309–312 (1997).
20. Stoytchev, M. & Genack, A. Z. Observations of non-Rayleigh statistics in the approach to photon localization. *Opt. Lett.* **24,** 262–264 (1999).
21. Garcia, N., Genack, A. Z. & Lisyansky, A. A. Measurement of the transport mean free path of diffusing photons. *Phys. Rev. B* **46,** 14475–14479 (1992).
22. Lagendijk, A., Vreeker, R. & de Vries, P. Influence of internal reflection on diffusive transport in strongly scattering media. *Phys. Lett. A* **136,** 81–88 (1989).
23. Garcia, N. & Genack, A. Z. Crossover to strong intensity correlation for microwave radiation in random media. *Phys. Rev. Lett.* **63,** 1678–1681 (1989).
24. Garcia, N., Genack, A. Z., Pnini, R. & Shapiro, B. Intensity correlation in waveguides. *Phys. Lett. A* **176,** 458–461 (1993).
25. Brouwer, P. W. Transmission through a many-channel random waveguide with absorption. *Phys. Rev. B* **57,** 10526–10531 (1998).
26. John, S. Strong localization of photons in certain disordered dielectric superlattices. *Phys. Rev. Lett.* **58,** 2486–2489 (1987).
27. Sigalas, M. M., Chan, C. T., Ho, K. M. & Soukoulis, C. M. Metallic photonic band-gap materials. *Phys. Rev. B* **52,** 11744–11751 (1995).
28. Stoytchev, M. & Genack, A. Z. Microwave transmission through a periodic three-dimensional metal-wire network containing random scatterers. *Phys. Rev. B* **55,** R8617–8621 (1997).
29. Arya, K., Su, Z. B. & Birman, J. L. Anderson localization of electromagnetic waves in a dielectric medium of randomly distributed metal particles. *Phys. Rev. Lett.* **57,** 2725–2728 (1986).
30. Condat, C. A. & Kirkpatrik, T. R. Observability of acoustical and optical localization. *Phys. Rev. Lett.* **58,** 226–229 (1987).

Acknowledgements

We thank P. W. Brouwer and E. Kogan for discussions. This work was supported by the NSF.

Correspondence and requests for materials should be addressed to A. A. C. (e-mail: achqc@qcunix1.acc.qc.edu).

Spontaneous macroscopic magnetization at the superconducting transition temperature of $YBa_2Cu_3O_{7-\delta}$

R. Carmi, E. Polturak, G. Koren & A. Auerbach

Physics Department, Technion–Israel Institute of Technology, Haifa 32000, Israel

A noteworthy feature of the high-temperature superconductors is the unconventional symmetry of the superconducting order parameter. Several experiments[1–3] have established that the order parameter has a four-fold $d_{x^2-y^2}$ symmetry under rotation of the lattice (the order parameter of conventional superconductors is, in contrast, isotropic). An intriguing and much debated possibility is that, in certain cases, an additional imaginary component might be present, having an isotropic *s*-wave[4–6] or d_{xy} symmetry[7–10]. A consequence of a complex order parameter of the form $d_{x^2-y^2}+id_{xy}$ is that it would break both reflection (parity, P) symmetry and time-reversal (T) symmetry, a clear signature of which would be the spontaneous appearance of a macroscopic magnetization at the superconducting transition temperature. Broken T symmetry has been reported[5,11], but searches for the effects of combined P and T symmetry breaking have so far yielded null results[12–15]. Here we report the observation of a weak ($\sim 10^{-5}$ gauss) magnetic field that appears spontaneously at the superconducting transition temperature of epitaxial thin films of $YBa_2Cu_3O_{7-\delta}$. The magnetic signal originates near the edges of the samples. One interpretation for this observation is that the order parameter carries an intrinsic angular momentum, related to the breaking of P and T symmetries, but other possibilities cannot yet be excluded.

Previous experimental searches of combined P and T violation set a limit of a few per cent on any symmetry-breaking component of the order parameter[12–15]. If a spontaneous magnetic field below this limit were to exist, it may be easier to detect it by looking at the magnetic flux produced by the whole sample, instead of a small region. This is conditional upon such a field having the same orientation everywhere in the superconductor. To check this possibility, in our experiment we placed high-quality epitaxial, *c*-axis-oriented $YBa_2Cu_3O_{7-\delta}$ films on top of an input coil of a d.c. SQUID (superconducting quantum interference device) magnetometer operating at 77 K (see Fig. 1a). The magnetometer (M2700L, Conductus, Inc.) has a large, 8 mm × 8mm directly coupled single input loop. The magnetometer is operated in a flux locked loop, with either a.c. or d.c. bias.

Films of $YBa_2Cu_3O_{7-\delta}$ were prepared either by laser ablation deposition or d.c. sputtering on 1 cm × 1 cm substrates, including (100)$SrTiO_3$, (100)MgO and (001)$NdGaO_3$. The range of thickness was between 30 nm and 300 nm, with the superconducting transition temperature, T_c, typically around 90 K. The films were measured as deposited, or after patterning into different structures

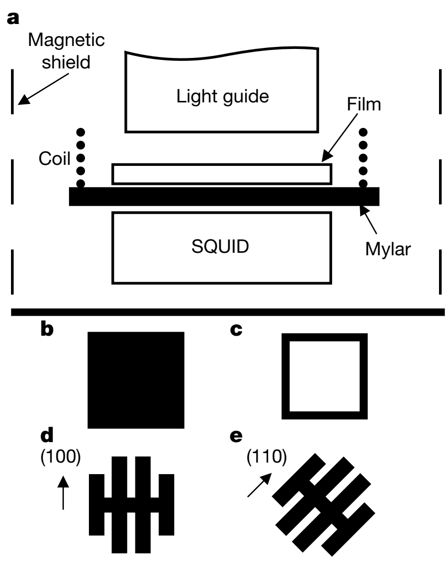

Figure 1 Schematic illustration of the experimental geometry and of the sample patterns. **a,** Cross-section of the experimental set-up. Light is introduced briefly through the light guide to heat the sample above T_c, and is turned off during the measurements. **b**–**e**, Film patterns used in this work. Magnetic shields reduce the residual field down to 10^{-4} G. Additional coils are used to further reduce this field, or to check for any field dependence. In order to avoid stray fields generated by currents used in resistive heating, the films are heated by a guided light beam; to eliminate any thermoelectric currents, the sample holder and all nearby components were made of non-magnetic plastic. Cooling of the samples is done using He exchange gas. The temperature of the films is measured *in situ* using the resistance of a carbon film painted onto the substrate. We verified that the small a.c. current used to measure the thermometer does not affect the results.

© 2000 Macmillan Magazines Ltd

described below. We have also tested pressed $YBa_2Cu_3O_{7-\delta}$ powder samples. In total, we measured 15 films, of which 14 showed spontaneous flux. Hence, the effect described here does not depend on the growth method or the substrate. In our measurement set-up shown in Fig. 1a, the distance between the sample and the SQUID is 1 mm. Despite the proximity, the film and the SQUID are located in two different chambers separated by a Mylar membrane, which allows us to vary the temperature of the films while keeping that of the SQUID constant at the base temperature of 77 K. We took care to reduce the residual magnetic field at the sample; see Fig. 1 legend for details. We verified, by changing the cooling rate by two orders of magnitude ($K\,s^{-1}$ to $K\,min^{-1}$) that the spontaneous signal was independent of thermal gradients.

Figure 2 shows a typical signal recorded by the magnetometer during the cooling of a film through T_c. A small spontaneous magnetic field appears abruptly at T_c, increasing in magnitude over an interval of about 1 K, and saturating below it. The ~1 K interval is typical of the spread of T_c across the wafer. Hence, the true interval is less than 1 K. The bottom part of Fig. 2 shows the reference measurement performed using a blank substrate. In order to ascertain that the effect is not caused by partial screening of the inductance of the SQUID as the sample cools through T_c, we inverted the film relative to the SQUID, and found that the polarity of the spontaneous signal was reversed (see Fig. 2 inset). A reversal of the signal rules out screening as a source of the effect. As an additional check, we measured the screening properties of the various film patterns (Fig. 1b–e) using a low-temperature inductance bridge. We found no correlation between the spontaneous signal and the screening properties. For example, the pressed powder samples had negligible screening relative to that of a film, while the spontaneous signal was 10–100 times larger. In addition, we ascertained that the bias polarity and the magnitude of the current in the feedback loop of the SQUID did not affect the signal (see Fig. 3 inset).

It is equally important to rule out external magnetic fields as a source of the effect. Any such field would be partially expelled from the film below T_c, inducing a signal proportional to the external field both in magnitude and sign. We repeated the measurements in the presence of magnetic fields up to 100 times larger than the residual field and along different directions. In a finite field, a temperature-dependent background appears below T_c, in addition to the spontaneous signal. An example of such measurement is shown in Fig. 3. Evidently, reversal of the external field between Fig. 3a and b changes the sign of the background, but not of the spontaneous signal such as shown in Fig. 2. The latter remains superimposed on this background, independent of both the magnitude and direction of the external field. This rules out the possibility that the effect originates from the presence of external fields or internal magnetic impurities. Comparing the data of Fig. 2 with that of Fig. 3, the weak temperature dependence seen below T_c in Fig. 2 is consistent with the presence of a residual field of $\sim 10^{-4}$ G. Consequently, the variation of the spontaneous field between T_c and 77 K is less than 10% of the jump at T_c.

We now consider the effects of sample geometry. In Fig. 4 we plot the size of the spontaneous field jump versus film thickness d. The comparison is made for unpatterned films (Fig. 1b), with identical areal dimensions. It is seen that, within the scatter, the signal does not depend on d. In the superconducting state, any magnetic moment appearing in the bulk of the film must be shielded by the Meissner effect. Net magnetic signal should therefore originate only from the edge of the film. We repeated the measurement after removing most of the film by lithography, leaving only a loop (Fig 1c). The magnitude of the signal coming from the loop did not change appreciably relative to the original film, which indicates that the magnetic signal originates near the edges. We also tested films patterned so that their edges were oriented along different crystalline directions, (100) or (110) (see Fig. 1d and e). We found that the signal did not depend on the orientation of the pattern, but in general, the magnitude of the signal increased with the length of the perimeter. This conclusion is further supported by data taken with pressed powder samples having much larger surface area than the films. In this case, the spontaneous signal was 10–100 times larger than shown in Fig. 2.

Our findings may be summarized as follows. First, after the initial

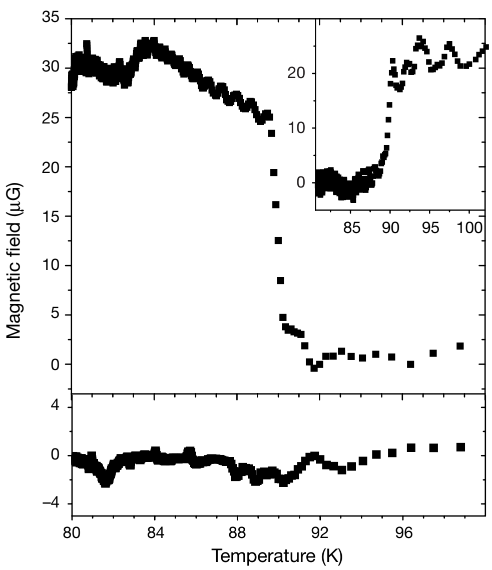

Figure 2 Spontaneous magnetic field generated by a thin YBCO film plotted against temperature. The sample is patterned as a disk, 0.7 cm in diameter. Inset, the signal measured after the film was inverted with respect to the SQUID. The magnitude of the signal in the main panel and in the inset is corrected for the different SQUID–sample distance—1 mm in the usual configuration and 2 mm with the film inverted. The bottom panel shows a reference measurement, done with a blank substrate.

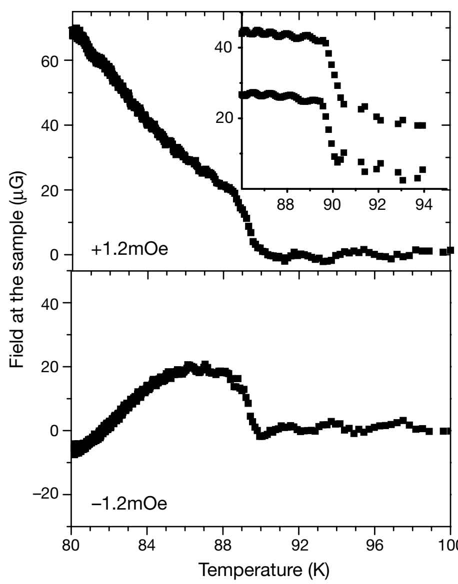

Figure 3 Total signal generated by a YBCO film cooled in an external magnetic field. The external field, 1.2 mG, is an order of magnitude larger than the residual field. Although the external field is reversed between the top and bottom parts of the figure, the spontaneous part of the signal appearing at T_c remains unchanged. Inset, the spontaneous signal at zero field obtained with reversed polarities of the SQUID bias. For clarity, the data were offset by a constant value.

© 2000 Macmillan Magazines Ltd

rise below T_c, the field picked up by the SQUID is independent of both temperature and film thickness. Second, the origin of the field is near the edges of the film. We examine two different models. (1) The effect is caused by an intrinsic angular momentum of the superconducting order parameter. (2) The film contains defects near its edges, which behave as internal π Josephson junctions.

Regarding model (1) we denote the intrinsic magnetization density by m_z. We assume that the flux emanates from a region of width W near the edge of perimeter length L. The flux measured by the SQUID is given by:

$$\Phi = \alpha 4\pi m_z WL \quad (1)$$

Here, α is the flux coupling coefficient between the sample and the SQUID. We determined α at about 0.5. Several authors[4,9] predict that magnetization related to P and T breaking should appear only within a coherence length ξ near defects or at surfaces, that is, $W = \xi$. There is no dependence on d. In order for these theories to explain also the temperature dependence of Φ, they should predict $m_z(T) \propto 1/\xi(T)$ which is also proportional to the gap Δ. For the data of Fig. 2, the flux generated by the sample is 7.7×10^{-6} G cm^{-2}, or 37 ϕ_0 (where $\phi_0 = hc/2e$). Extrapolating to $T = 0$, and using $\xi_0 = 15$ Å, we find the edge field (inside a width ξ_0) would be 23 G. Fields of this magnitude were suggested in ref. 9.

Another possibility is that the intrinsic magnetization is a property of the bulk[7,8]. However, a non-zero magnetic signal would come only from a region of width $W = \lambda_{eff}$ which is not shielded by the Meissner effect[7]. In the case of a thin film, $\lambda_{eff} = \lambda^2/d$, where λ is the London penetration depth[16]. This relation holds for $d < \lambda$ which is always true near T_c. In this case, $m_z(T)$ should be proportional to d/λ^2 to cancel the temperature and thickness dependence of Φ. Thus, to be in line with our data, the predicted $m_z(T)$ should be proportional to the areal superfluid density. Extrapolating to $T = 0$, and using $\lambda_0 = 1{,}400$ Å, and $d = 2{,}500$ Å, we find the edge field (inside a width λ_0^2/d) would be 0.37 G for the sample of Fig. 2. If one looks at the edge area using a SQUID microscope with a 10 μm $\times$ 10 μm pickup loop[17], the average field sensed would be about 10^{-3} G for both cases ($W = \xi_0$ or $W = \lambda_0^2/d$). Edge fields of this magnitude were indeed observed[17].

From the results, we set limits on the intrinsic magnetic moment per plaquette. A plaquette is a section of a CuO_2 plane of unit cell size. If $W = \xi_0$, we calculate from equation (1) a magnetic moment of 1.8×10^{-2} μ_B per CuO_2 plaquette (here μ_B is the Bohr magneton). In the case of $W = \lambda_0^2/d$, we get 3.7×10^{-4} μ_B per CuO_2 plaquette. If one further assumes that m_z reflects the intrinsic orbital moment density of the Cooper pairs, we can convert it to an intrinsic angular momentum per Cooper pair $\langle L_z \rangle$. Assuming a pair density of 0.08 per CuO_2 plaquette (half of the hole density), and an orbital magnetic moment of 4 $\mu_B \langle L_z \rangle/h$ per pair, we obtain $\langle L_z \rangle/h = 1.2 \times 10^{-3}$ if $W = \lambda_0^2/d$ and $\langle L_z \rangle/h = 6 \times 10^{-2}$ if $W = \xi_0$. This implies $\Delta_{xy}/\Delta_{x^2-y^2} \approx 5 \times 10^{-4}$ for $W = \lambda_0^2/d$ and $\Delta_{xy}/\Delta_{x^2-y^2} \approx 2.5 \times 10^{-2}$ if $W = \xi_0$. Thus, the d_{xy} component is very small, which may explain why it went undetected until now.

Turning to model (2), it is well known that spontaneous flux of $\phi_0/2$ appears in a superconducting loop containing a π junction[1,2,18,19]. The flux coming from the sample in Fig. 2 could be generated by 74 junctions with circulating currents all in the same sense. This would explain the jump at T_c, and the temperature and thickness independence below T_c. The fact that the signal originates near the edges implies that such junctions are perhaps associated with defects near the boundary. There are however several points which are unclear regarding this interpretation. First, large-angle grain boundaries which are usually used to construct π junctions[2] are absent in epitaxial films. Thus, one has to look for defects of another kind. Second, removing the original boundary of the film by patterning did not change the signal size appreciably. Third, the total flux measured seems to be the same in different films (Fig. 4). This requires that the number of spontaneously created vortices and their sign is not random.

We note that the inset in Fig. 2 and the main panel of Fig. 3 show that the direction of the spontaneous field is robust with respect to small external fields and temperature cycling. But this direction, although seemingly fixed for each sample, was random between different samples. This suggests that the direction of this field is determined at temperatures above room temperature, certainly higher than T_c. □

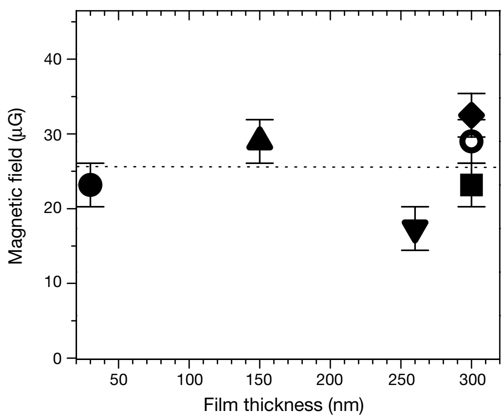

Figure 4 Magnitude of the spontaneous field jump plotted against film thickness. The various symbols are used only for sample identification. Error bars reflect the noise level in the data, while the dashed line is the average value of the signal.

Received 23 September 1999; accepted 11 February 2000.

1. Wollman, D. A, Van Harlingen, D. J., Giapintzakis, J. & Ginsberg, D. M. Evidence for $d_{x^2-y^2}$ pairing from magnetic field modulation of YBCo-Pb Josephson junctions. *Phys. Rev. Lett.* **74,** 797–800 (1995).
2. Tsuei, C. C. *et al.* Pairing symmetry in single layer $Tl_2Ba_2CuO_{6+\delta}$. *Science* **271,** 329–332 (1996).
3. Shen, Z. X. *et al.* Anomalously large gap anisotropy in the a-b plane of $Bi_2Sr_2CaCuO_8$. *Phys. Rev. Lett.* **70,** 1553–1556 (1993).
4. Sigrist, M. Time reversal symmetry breaking states in high temperature superconductors. *Prog. Theor. Phys. (Jpn)* **99,** 899–929 (1998).
5. Covington, M., Aprili, M., Paraoanu, E. & Greene, L. H. Observation of surface induced broken time reversal symmetry in $YBa_2Cu_3O_{7-\delta}$ tunnel junctions. *Phys. Rev. Lett.* **79,** 277–281 (1997).
6. Fogelstrom, M., Rainer, D. & Sauls, J. A. Tunneling into current carrying states of high T_c superconductors. *Phys. Rev. Lett.* **79,** 281–284 (1997).
7. Halperin, B. I., March-Russell, J. & Wilczek, F. Consequences of time reversal symmetry violation in models of high T_c superconductors. *Phys. Rev. B* **40,** 8726–8744 (1989).
8. Laughlin, R. B. Magnetic induction of $d_{x^2-y^2} + id_{xy}$ order in high T_c superconductors. *Phys. Rev. Lett.* **80,** 5188–5191(1998).
9. Salkola, M. I & Schrieffer, J. R. Unusual states of inhomogeneous $d_{x^2-y^2} + id_{xy}$ superconductors. *Phys. Rev. B* **58,** R5952–R5255 (1998).
10. Krishana, K, Ong, N. P., Li, Q., Gu, G. D. & Koshizuka, N. Plateaus observed in the field profile of thermal conductivity in the superconductor $Bi_2Sr_2CaCu_2O_8$. *Science* **277,** 83–85 (1997).
11. Krupke, R. & Deutscher, G. Anisotropic magnetic field dependence of zero bias anomaly of in-plane oriented (100) $Yba_2Cu_3O_{7-\delta}$/In tunnel junctions. *Phys. Rev. Lett.* **83,** 4634–4637 (1999).
12. Kiefl, R. F. *et al.* Search for anomalous internal fields in high T_c superconductors as evidence for broken time reversal symmetry. *Phys. Rev. Lett.* **64,** 2082–2085 (1990).
13. Spielman, S. *et al.* Measurement of the spontaneous Kerr effect in $Bi_2Sr_2CaCuO_8$. *Phys. Rev. Lett.* **68,** 3472–3475 (1992).
14. Mathai, A., Gim, Y., Black, R. C., Amar, A. & Wellstood, F. C. Experimental proof of time reversal invariant order parameter with a π shift in $YBa_2Cu_3O_{7-\delta}$. *Phys. Rev. Lett* **74,** 4523–4526 (1995).
15. Kirtley, J. R., Tsuei, C. C. & Moler, K. A. Temperature dependence of the half-integer magnetic flux quantum. *Science* **285,** 1373–1375 (1999).
16. Pearl, J. Current distribution in superconducting films carrying quantized fluxoids. *Appl. Phys. Lett.* **5,** 65–66 (1964).
17. Kirtley, J. R. *et al.* Distribution of magnetic flux in high T_c grain-boundary junctions enclosing hexagonal and triangular areas. *Phys. Rev. B* **51,** 12057–12060 (1995).
18. Sigrist, M. & Rice, T. M. Paramagnetic effect in high T_c superconductors-a hint for d-wave superconductivity. *J. Phys. Soc. Jpn* **61,** 4283–4286 (1992).
19. Kawamura, H. & Li, M. S. Equilibrium phase with broken time reversal symmetry in ceramic high T_c superconductors. *Phys. Rev. Lett.* **78,** 1556–1559 (1997).

Acknowledgements

We thank E. Zeldov for discussions. This work was supported by the Israel Science Foundation, The Heinrich Hertz Minerva Center for HTSC, and by the VPR Technion Fund for Promotion of Research.

Correspondence and requests for materials should be addressed to E. P. (e-mail: emilp@physics.technion.ac.il).

© 2000 Macmillan Magazines Ltd